

Supporting Information

# Stabilizing Interface Between $\text{Li}_2\text{S-P}_2\text{S}_5$ Glass-Ceramic Electrolyte and Ether Electrolyte by Tuning Solvation Reaction

Bo Fan<sup>†,‡,§</sup>, Wenzhi Li<sup>†</sup>, Zhongkuan Luo<sup>||</sup>, Xianghua Zhang<sup>⊥</sup>, Hongli Ma<sup>⊥</sup>,  
Ping Fan<sup>‡</sup>, Bai Xue<sup>\*,‡</sup>

<sup>†</sup> College of Materials Science and Engineering, Shenzhen University, 518060 Shenzhen, China

<sup>‡</sup> Shenzhen Key Laboratory of Advanced Thin Films and Applications, College of Physics and Optoelectronic Engineering, Shenzhen University, 518060 Shenzhen, China

<sup>§</sup> State Key Lab of Silicon Materials, Zhejiang University, Hangzhou 310027, China

<sup>||</sup> College of Chemistry and Environmental Engineering, Shenzhen University, 518060 Shenzhen, China

<sup>⊥</sup> Laboratory of Glasses and Ceramics, Institute of Chemical Science, University of Rennes 1, Rennes 35042, France

\* Corresponding author: [baixue@szu.edu.cn](mailto:baixue@szu.edu.cn)

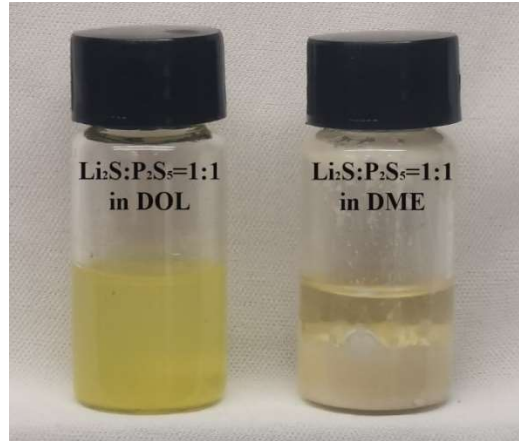


Figure S1. Photograph of a  $\text{Li}_2\text{S}-\text{P}_2\text{S}_5$  mixture (molar ratio 1:1) after 5 days of immersion in DOL and DME, respectively.

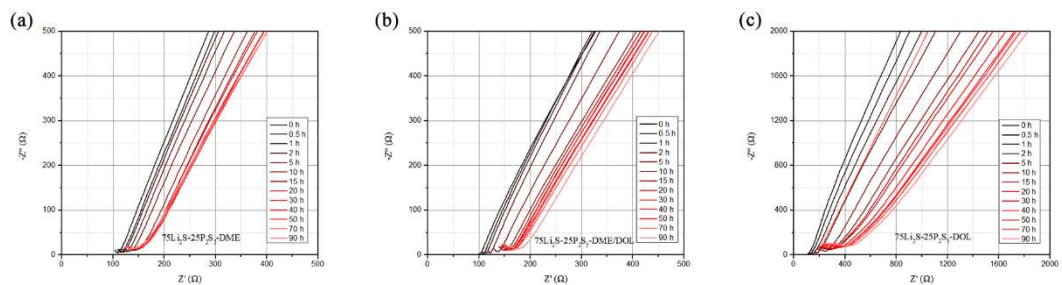


Figure S2. Temporal evolution of the impedance spectra of the  $75\text{Li}_2\text{S}-25\text{P}_2\text{S}_5$  glass-ceramic pellets in contact with the ether-based liquid electrolytes. (a) DME, (b) DME/DOL, (c) DOL.

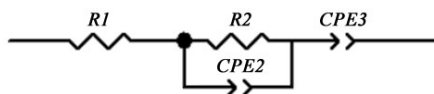


Figure S3. Equivalent circuit used to fit the impedance spectra in Figure S2.

Table S1. Fitting parameters for the impedance spectra in Figure S2a.

Time (h)	$R1$ ( $\Omega$ )	$R2$ ( $\Omega$ )	$CPE2-T$ ( $F s^{p-1}$ )	$CPE2-P$	$CPE3-T$ ( $F s^{p-1}$ )	$CPE3-P$
0	85.6	26.0	2.2E-07	0.75	1.2E-05	0.78
1	85.6	36.3	4.3E-07	0.67	1.4E-05	0.77
3	85.6	48.7	9.1E-07	0.61	1.4E-05	0.76
5	85.6	52.1	2.1E-06	0.55	1.4E-05	0.76
10	85.6	68.2	7.4E-06	0.47	1.4E-05	0.75
15	85.6	77.3	1.4E-05	0.42	1.4E-05	0.74
20	85.6	80.3	1.9E-05	0.41	1.5E-05	0.74
30	85.6	82.2	2.1E-05	0.41	1.5E-05	0.73
40	85.6	80.6	2.0E-05	0.41	1.6E-05	0.72
50	85.6	81.0	2.8E-05	0.39	1.6E-05	0.72
70	85.6	80.4	2.2E-05	0.41	1.6E-05	0.72
90	85.6	81.4	2.7E-05	0.41	1.6E-05	0.72

Table S2. Fitting parameters for the impedance spectra in Figure S2b.

Time (h)	$R1$ ( $\Omega$ )	$R2$ ( $\Omega$ )	$CPE2-T$ ( $F s^{p-1}$ )	$CPE2-P$	$CPE3-T$ ( $F s^{p-1}$ )	$CPE3-P$
0	73.4	28.6	1.2E-09	0.95	2.9E-05	0.75
1	73.4	40.1	5.7E-09	0.87	1.9E-05	0.75
3	73.4	53.9	6.1E-09	0.86	1.6E-05	0.74
5	73.4	62.9	6.6E-09	0.86	1.6E-05	0.72
10	73.4	76.1	8.2E-09	0.81	1.6E-05	0.70
15	73.4	82.4	1.9E-08	0.79	1.6E-05	0.69
20	73.4	86.8	2.9E-08	0.76	1.5E-05	0.69
30	73.4	89.2	5.4E-08	0.72	1.5E-05	0.69
40	73.4	91.7	1.0E-07	0.68	1.5E-05	0.69
50	73.4	94.9	1.8E-07	0.64	1.6E-05	0.69
70	73.4	105.3	1.4E-06	0.48	1.1E-05	0.69
90	73.4	110.4	1.2E-06	0.48	1.1E-05	0.69

Table S3. Fitting parameters for the impedance spectra in Figure S2c.

Time (h)	$R1$ ( $\Omega$ )	$R2$ ( $\Omega$ )	$CPE2-T$ ( $F s^{p-1}$ )	$CPE2-P$	$CPE3-T$ ( $F s^{p-1}$ )	$CPE3-P$
0	84.4	28.4	2.8E-09	0.99	1.4E-05	0.70
1	84.4	66.7	3.3E-09	0.92	1.5E-05	0.68
3	84.4	127.9	7.5E-08	0.71	1.1E-05	0.69
5	84.4	173.8	3.0E-07	0.62	1.1E-05	0.67
10	84.4	221.4	5.8E-07	0.58	1.2E-05	0.67
15	84.4	235.4	5.8E-07	0.58	1.7E-05	0.60
20	84.4	247.2	5.6E-07	0.58	1.5E-05	0.61
30	84.4	287.8	4.8E-07	0.58	1.7E-05	0.59
40	84.4	317.2	4.5E-07	0.59	1.8E-05	0.59
50	84.4	336.3	4.2E-07	0.59	1.8E-05	0.58
70	84.4	364.2	4.0E-07	0.59	1.9E-05	0.58
90	84.4	372.4	3.9E-07	0.59	1.9E-05	0.57

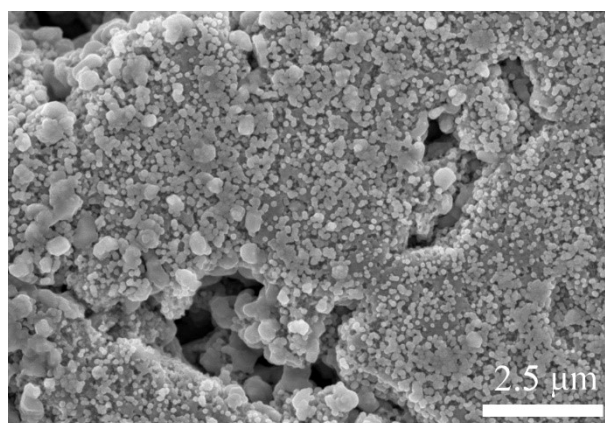


Figure S4. Top-view SEM image of the pristine 75Li<sub>2</sub>S-25P<sub>2</sub>S<sub>5</sub> pellet.

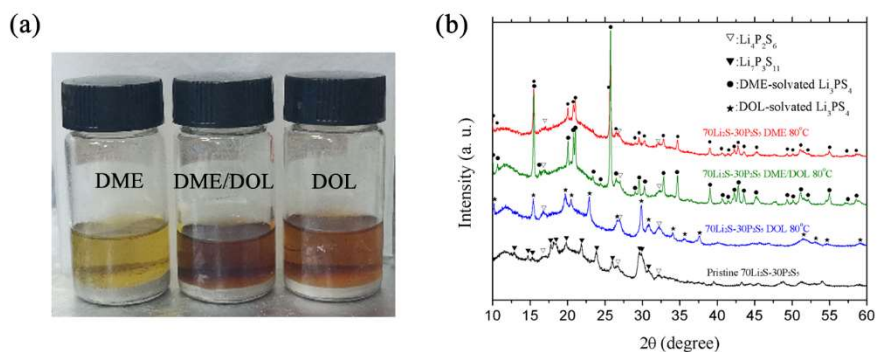


Figure S5. (a) Photographs of the  $70\text{Li}_2\text{S}-30\text{P}_2\text{S}_5$  glass-ceramic powders after 48 h of immersion in DME, DOL, and DME/DOL (50–50 vol.%). The deeper color of the supernatant than that of the  $75\text{Li}_2\text{S}-25\text{P}_2\text{S}_5$  glass-ceramic implied that the corrosion was more severe for the  $70\text{Li}_2\text{S}-30\text{P}_2\text{S}_5$  glass-ceramic. (b) XRD patterns of the 48-h-immersed  $70\text{Li}_2\text{S}-30\text{P}_2\text{S}_5$  powder in different solvents, after  $80^\circ\text{C}$  drying. It shows that the  $\text{Li}_7\text{P}_3\text{S}_{11}$  phase in the pristine sample was decomposed by the ether solvents into the solvated  $\text{Li}_3\text{PS}_4$ .

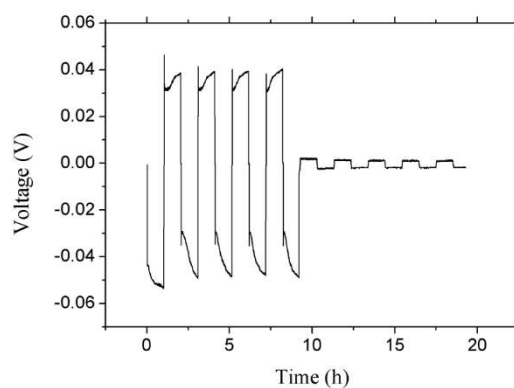


Figure S6. Voltage profile of the lithium plating/stripping cycling in an all-solid-state Li symmetric cell with a structure of  $\text{Li}/\text{Li}_2\text{S}-\text{P}_2\text{S}_5/\text{Li}$ . The current density was  $0.36\text{ mA cm}^{-2}$ .

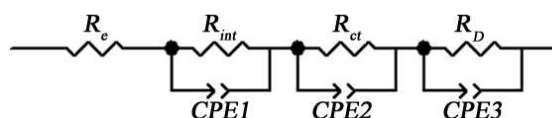


Figure S7. Equivalent circuit used to fit the electrochemical impedance spectra of the Li/LE/SE/LE/Li symmetric cells in Figure 4. The curved low-frequency tail was roughly fitted by  $R_D//CPE3$  for convenience. This simplified treatment does not affect the fitting accuracy of  $R_e$ ,  $R_{int}$ , and  $R_{ct}$  owing to the separation of their time constants.

Table S4 Internal resistances of the Li/LE/SE/LE/Li symmetric cells extracted from the electrochemical impedance spectra in Figure 4 by equivalent-circuit fitting.

Solvent		$R_e$ ( $\Omega$ )	$R_{int}$ ( $\Omega$ )	$R_{ct}$ ( $\Omega$ )
DME	5 cyc	32	11	14
	100 cyc	34	17	5
DME/DOL	5 cyc	28	9	9
	100 cyc	31	17	4
DOL	5 cyc	57	18	7
	25 cyc	99	54	6
	30 cyc	194	12213	305

Table S5. Elemental analysis of the cycled S-C cathodes using the DME/DOL-based LE and DOL-based LE, respectively. The higher P content in the DOL sample than that in the DME/DOL sample indicates that the thin film covering the cathode in Figure 5h is rich in P.

solvent	C (wt.%)	O (wt.%)	S (wt.%)	P (wt.%)	F (wt.%)
DME/DOL	25.6	14.2	42.6	3.1	14.5
DOL	22.1	7.7	51.8	6.8	11.6